



Acid modified natural clay as a judicious solution for the successive treatment of ametryn

S.F.A. Shattar, N.A. Zakaria, K.Y. Foo*

River Engineering and Urban Drainage Research Centre (REDAC), Engineering Campus, Universiti Sains Malaysia, Seri Ampangan 14300 Nibong Tebal, Penang, Malaysia, Tel. +6045996539, Fax +6045996926, email: k.y.foo@usm.my (K.Y. Foo)

Received 10 January 2017; Accepted 20 January 2018

ABSTRACT

In this study, a locally sourced clay was harnessed and modified as a renewable and low cost adsorbent. The modified clay (ANC) was subjected to the evaluation of morphological structure, detection of surface functional groups, and nitrogen adsorption-desorption test. The adsorptive potential was examined for the effective treatment of ametryn. Equilibrium data were simulated using the Langmuir, Freundlich, Temkin and Redlich-Peterson isotherms models. Adsorption kinetic was fitted to the pseudo-first order, pseudo-second order and Elovich kinetic equations, while the adsorption mechanism was established by the intraparticle diffusion model. The newly prepared ANC demonstrated the high specific surface area, Langmuir surface area and total pore volume of 43.34 m²/g, 55.80 m²/g, and 0.120 cm³/g, respectively, verified by the Scanning Electron Micrograph and Fourier Transform Infrared Spectroscopy. The adsorption data was satisfactory described by the Langmuir isotherm model, with a monolayer adsorption capacity for ametryn of 85.16 mg/g. The adsorption kinetic was best confronted to the pseudo-second order model, suggesting chemisorption is the rate limiting step. The findings supported the viability of ANC as a promising and economical solution for the successive remediation of pesticide contaminated agricultural runoff.

Keywords: Acid modification; Adsorption; Ametryn; Natural clay; Pesticide

1. Introduction

Concern about environmental preservation has increased over the years from a global view point. Today, the indiscriminate discharge of organo-pesticide, specifically ametryn into surface water and marine coastal environment is dictated to be a primary agenda by the environmental practitioners. Ametryn is a herbicide of the triazine family, with a chemical structure of the aromatic hexamer ring. The annual application of active ametryn is 380,000 lbs. Dormant seasonal application of ametryn in conjunction with frequent rainfall may result in the generation of contaminated runoff and offsite environmental risks. A typical mechanism for the ametryn pollution is driven by the agricultural run-off during the storm events. Schiff and Sutula [1] have reported that during the rain events, the pesticide transport to the receiving waterways may

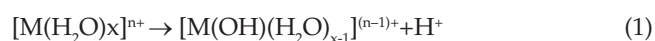
enhance the flow from < 0.03 to > 283.2 m³/s. According to Bucheli et al. [2], the average concentration for the single rain events and total loads for triazines was 903 ng/L and 13,900 ng/m²-y, respectively. This transient movement however, is highly dependent on the soil type and retention by the solid organo-mineral phase [3,4]. In the perspective, a critical approach to retard the migration of ametryn is by the adsorption of ametryn onto the clay minerals.

Clays are hydrous aluminosilicates that make up the colloidal fraction (<2 μm) of soils, sediments, rocks and water, and may be composed of the mixtures of fine grained minerals, crystals of quartz, carbonate and metal oxides [5]. Due to their abundant availability in nature, clays have found wide applications in the manufacture of pottery and ceramics, and serve as the medicinal and therapeutic agents, among which Bolus Armenus (a red clay from Cappadocia) and terra sigillata (a kaolinite-riched material from the island of Lemnos) are well known for their efficacy in curing festering wounds, skin afflictions, and snake bites

*Corresponding author.

[6–8]. Likewise, Sudanese villagers along the Nile have traditionally applied local bentonite against the viruses and bacteria of river water [9,10]. These practical applications rely primarily on the ability of these minerals to adsorb and retain harmful and undesirable substances from the natural environment, and the adsorptive capability of natural clays is related to their particle size, specific surface area, layer structure, and charge characteristics. The vast literature on the interactions of clay minerals, with the small and polymeric organic molecules has periodically been reviewed [11–14].

The prominent cations and anions found on the clay surface are Ca^{2+} , Mg^{2+} , H^+ , K^+ , NH_4^+ , Na^+ and SO_4^{2-} , Cl^- , PO_4^{3-} , and NO_3^- , which could be exchanged with other ions easily without affecting the mineral structure. Both Brönsted and Lewis type of acidity would boost the adsorption capacity of clay minerals to a great extent [15]. The Brönsted acidity, arises from the H^+ ions are formed by the dissociation of water molecules of hydrated exchangeable metal cations on the surface derived as:



It may also arise from the net negative charge of the clay structure, mainly ascribed to the substitution of Si^{4+} by Al^{3+} in some of the tetrahedral positions, and the resultant charge is balanced by the H_3O^+ cations. The Lewis acidity may derive from the exposure to trivalent cations, mostly Al^{3+} at the edges, Al^{3+} from the rupture of Si-O-Al bonds, or through dehydroxylation of some Brönsted acid sites. The edges and the faces of these clay particles could adsorb anions, cations, non-ionic and polar contaminants in the natural water via the processes of ion exchange, coordination, and ion-dipole moments, or H-bonding, van der Waals and hydrophobic interactions. The strength of these interactions is determined by various structural behaviour and other unique features of the clay minerals. van Olphen [16] has cited several types of active sites in clays, viz., (i) Brönsted acid or proton donor sites, created by the interactions of adsorbed or interlayer water molecules, (ii) Lewis acid or electron acceptor sites due to dehydroxylation, (iii) oxidizing sites, due to the presence of some cations in octahedral positions, or due to the adsorbed oxygen on the surfaces, (iv) reducing sites due to the presence of Fe^{2+} ions, and (v) surface hydroxyl groups, mostly found in the edges, bounded to Si, Al or other octahedral cations [17]. The interaction to retain harmful and undesirable substances from their immediate environment has surged to a variety of applications [18]. Although the reactivity of these minerals might be expected to extent to a broad range of anthropogenic and industrial pollutants, these clay minerals have shown limited applications in their natural state [19–21].

In this sense, the presence research was carried out to investigate the potential of natural clay, abundantly available from the plantation area as a suitable substitute to commercial adsorbents for the innovative treatment of ametryn, a highly hazardous pesticide from the aqueous solution in a batch mode study. The initial raw precursor was treated by acid leaching with sulphuric acid to reduce the clay crystallinity. Structural, functional, and surface chemistry of the newly prepared clay based adsorbent were evaluated by Fourier transform infrared (FTIR) spec-

troscopy, scanning electron microscopy (SEM), nitrogen adsorption-desorption curve and zero point of charge. The experimental parameters, initial concentration, contact time, and solution pH on the adsorption behaviour were examined. The adsorption data were analyzed on the basis of the Langmuir, Freundlich, Temkin and Redlich-Peterson isotherm models, while the kinetic equilibrium, adsorption mechanism and thermodynamics analysis were elucidated.

2. Materials and methods

2.1. Materials

The natural clay (NC) acquired from a paddy field, was chosen as the initial raw precursor in this work. The clay sample was stirred vigorously at 90°C in 6% of hydrogen peroxide solution or 2 N of acetic acid solution for the elimination of organic and carbonaceous impurities [25]. The resulting sample was washed thoroughly with distilled water, and dried at 105°C. The dried sample was crushed, ground, and sieved to the particle size of 20–45 µm. Ametryn, with a chemical formula of $\text{C}_9\text{H}_{17}\text{N}_5\text{S}$, and molecular weight of 227.33 g/mole, was applied as the model adsorbate. All the reagents used in this study were of analytical grade. Deionized water was used to prepare all the solutions and reagents.

2.2. Preparation of adsorbent

The preparation of clay-based adsorbent was performed by the immersion of 10 g of clay micro-powder in 40 mL of sulphuric acid solution (9 M) under mechanical stirring at 200 rpm and 75°C for 3 h. The resulting sample was rinsed with hot distilled water until pH 6–7 was achieved in the washing solution. The obtained adsorbent (ANC) was dried at 60°C for 24 h and stored in a sealed container prior to be used.

2.3. Batch adsorption studies

The batch adsorption experiments were undertaken in a set of 250 mL Erlenmeyer flasks containing 0.20 g of adsorbent and 200 mL of ametryn solutions within the concentration range of 25–150 mg/L. The mixture was agitated at 120 rpm in an isothermal water-bath shaker until the equilibrium was reached. For the kinetic study, the ametryn concentrations in the supernatant solutions were withdrawn at pre-determined period, and measured using a double beam UV-vis spectrophotometer (UV-1800 Shimadzu, Japan) at 224 nm. All samples were filtered prior to analysis. Each experiment was duplicated under identical conditions. The adsorptive uptake of ametryn at time t , q_t (mg/g) and equilibrium, q_e (mg/g), was calculated by:

$$q_t = \frac{(C_0 - C_t)V}{W} \quad (2)$$

$$q_e = \frac{(C_0 - C_e)V}{W} \quad (3)$$

where C_0 , C_t and C_e (mg/L) are the liquid-phase concentrations of ametryn solution at initial, time t (min) and equilib-

rium, respectively. V (L) is the volume of the solution, and W (g) is the mass of adsorbent.

The effect of solution pH on the ametryn removal was examined by regulating the solution pH from 2 to 12, with an initial ametryn concentration of 100 mg/L, ANC dosage of 0.20 g/200 mL and adsorption temperature of 30°C. The initial pH of the ametryn solution was adjusted by the addition of 0.10 M of hydrochloric acid (HCl) or sodium hydroxide (NaOH) solution. The pH was measured using a pH meter (Accumet XL200, Fischer Scientific).

2.4. Physical and chemical characterization

The surface morphology was examined using the Zeiss Supra 35VP scanning electron microscope with an accelerating voltage of 15 kV and a vacuum of 10^{-5} Pa. During the operation, the samples were coated with a thin layer of gold, placed into the chamber, and transferred to the path of electron beam prior to the scanning process. Fourier Transform Infrared (FTIR) Spectroscopy was carried out using the FTIR spectrometer Vertex 80v equipped by DTGS detector and KBr beam-splitter (Bruker, Ettlingen, Germany). The samples were prepared as pressed KBr-pellets, which 0.5 mg of clay samples were dispersed in 200 mg of KBr. The mixture was placed in a 13 mm pellet disk and pressed in vacuum. The adsorption spectra were recorded in the wavelength range from 4000–400 cm^{-1} with 256 scans, and a resolution of 4 cm^{-1} . Baseline correction was performed by Concave Rubberband method, with 64 baseline points and 10 iterations.

The pore structural characteristics were determined by nitrogen adsorption-desorption curve at 77 K using an automatic Micromeritics ASAP-2020 volumetric adsorption analyzer. The specific surface area was calculated by the Brunauer-Emmett-Teller (BET) equation; the total pore volume was evaluated by converting the adsorption volume of nitrogen at relative pressure of 0.95 to equivalent liquid volume of the adsorbate, while the micropore volume, micropore surface area and external surface area were obtained using the t -plot method.

2.5. Zero point of charge (pH_{pzc})

The determination of zero point of charge (pH_{pzc}) was performed by adjusting the pH of 50 mL of the 0.01 M sodium chloride (NaCl) solution from 2 to 12. 0.15 g of ANC was added into the flasks, and the suspensions were mixed for 48 h. The final solution pH (pH_f) was measured, and the pH_{pzc} of the tested adsorbent was obtained by plotting pH_f versus pH_i . The pH at which the final pH (pH_f) curve cuts the initial pH (pH_i) line was denoted as the pH_{pzc} .

3. Results and discussion

3.1. Batch adsorption studies

The effect of initial concentration and contact time on the adsorptive uptake of ametryn onto ANC is displayed in Fig. 1a. Initial concentration provides an important driving force for alleviating mass transfer resistance between the aqueous phase and the solid medium [26]. Increasing initial

concentration from 25 to 150 mg/L showed an enhancement of the adsorption uptake of ametryn from 12.49 to 50.12 mg/g, mainly ascribed to the higher concentration gradient which governs the adsorption process. The time profile of ametryn uptake is a single, smooth and continuous curve leading to saturation, suggesting possible monolayer coverage of ametryn onto the surface of ANC. Additionally, the adsorptive uptake and removal of ametryn increased with prolonging the contact time. The adsorption process increased sharply at the initial stage, indicating the availability of readily accessible sites. The process was gradually slowed down as the equilibrium approached [27]. Similar result was obtained for the adsorption of cationic dye by clay [28] and the adsorption of malachite green onto montmorillonite [29].

Solution pH has a significant effect on the adsorptive uptake of the adsorbate, since it determines the surface charge, and the degree of ionization and speciation of the adsorbate in the aqueous solution [30]. The effect of solution pH was investigated by varying the pH of ametryn solutions from 2 to 12, with an initial concentration of 100 mg/L, as shown in Fig. 1b. Decreasing solution pH exerted a significant enhancement on the adsorptive

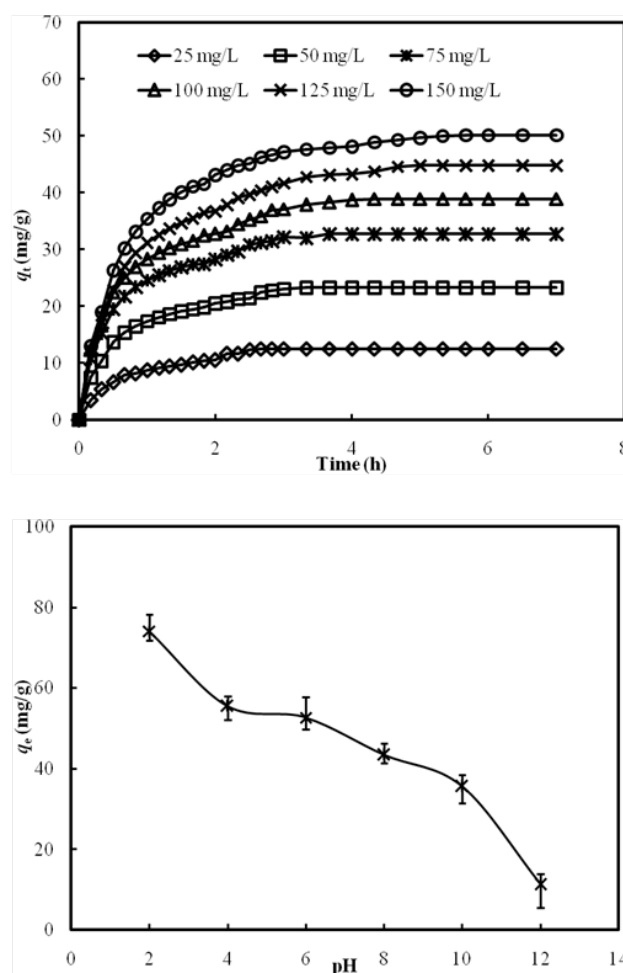


Fig. 1. Effect of (a) initial concentration and contact time and (b) solution pH on the adsorptive uptake of ametryn onto ANC at 30°C.

uptake of ametryn from 11.28 to 74.10 mg/g. High adsorption uptake at strong acidic pH is due to the protonation of the ametryn molecules. Similar observation was illustrated by the adsorption of *s*-triazines onto montmorillonite. Weber [31] has related the molecular structure of *s*-triazine to their adsorption capacity at the pH range of 1–10. The maximum adsorption occurred at the solution pH near to the pK_a of the adsorbate. In another study conducted by Ahmad et al. [32], the adsorption of ametryn showed a greater capacity at the solution pH below 6, with the k_d values ranging between 20.45–47.62. At the pH values near to the pK_a of ametryn (4.0), decreasing pH would induce the protonation of ametryn, and the resulting cations would be adsorbed to the negatively charged soil colloid [33]. This protonated ametryn held on the negatively charged clay minerals to resist the desorption process. Yamane and Green [34] also found that, the adsorption of ametryn onto montmorillonite was attributed to the degree of protonation at low solution pH, and polarizability property at the highly basic medium. Due to the protonation of isopropylamine and ethylamine groups at the lower solution pH, ametryn molecules would present predominantly in positively charged (cationic) at the solution pH < 4.1, and in the molecular form at the solution pH > 4.1 [35]. Comparative study for the adsorption of triazine onto montmorillonite has demonstrated that higher adsorption was found as the solution pH approaches to the pK_a of the solute compound [36,37], with the formation of cation at pH < pK_a , and at the pH > pK_a , ametryn was in the molecular (neutral) form.

Moreover, the pH_{pzc} of ANC has been identified to be 3.71. Generally, the main contribution to the surface charge of ANC is the permanent negative charge on the basal planes due to the isomorphous substitutions [38]. The negative charge associated with cation replacement in the tetrahedral sheet (Al^{3+} for Si^{4+}) may result in localized charge distribution, with larger diffuse negative charge from the cation replacement in the octahedral sheets (Mg^{2+} for Al^{3+}) [39]. This excess of negative lattice charge is compensated by the exchangeable cations in the diffuse part of the dominant electric double layer on faces. Additional polarity, mainly octahedral Al-OH and tetrahedral Si-OH groups, are situated at the broken edges of the clay minerals. These amphoteric sites are conditionally charged, and could be developed at the edges by H^+ or OH^- transfer from the aqueous phase.

Therefore, at the acidic pH, the surface of ANC would be protonated and turned into positively charged to form a dominant and hidden electric double layer around the ANC lamellae. This positive charge could be developed only on the Al-OH sites of edges at the pHs below 3.71. At the pH equal to the pH_{pzc} , the surface of ANC was essentially neutral, to induce weakening of the surface interaction with the ametryn molecules, and reduced the degree of adsorption onto the functionalized adsorbent. Conversely, the unique surface heterogeneity of ANC lamellae could disappear, if the pH of the suspensions is well above the pH_{pzc} , mainly ascribed to the deprotonation of Si-OH, resulting in the repulsive interaction between ANC and ametryn molecules [40].

3.2. Adsorption isotherm

Adsorption equilibrium is established when an adsorbate-containing phase has been contacted with the adsorbent for sufficient time, and the adsorbate concentration in the bulk solution is in a dynamic balance with the interface concentration [41]. An adsorption isotherm describes the interaction between the adsorbates molecules with the solid adsorbents. The Langmuir [42], Freundlich [43], Temkin [44] and Redlich-Peterson [45] isotherm models are among the simplest, and most commonly applied isotherm models to represent the adsorption of adsorbate molecules from the liquid phase onto a solid adsorbent, derived as:

$$q_e = \frac{Q_0 K_L C_e}{1 + K_L C_e} \quad (4)$$

$$q_e = K_F C_e^{1/n} \quad (5)$$

$$q_e = \frac{RT}{b_T} \ln A_T C_e \quad (6)$$

$$q_e = \frac{k_R C_e}{1 + a_R C_e^\beta} \quad (7)$$

where Q_0 (mg/g) and K_L (L/g) are the Langmuir isotherm constants related to adsorption capacity and rate of adsorption, whereas K_F (mg/g)·(L/mg) $^{1/n}$ is the Freundlich isotherm constant related to the distribution coefficient representing the quantity of ametryn adsorbed per unit of equilibrium concentration, and n provides an indication on the favourability of the adsorption process. $B = RT/b_T$, where b_T , A_T , R and T are the Temkin isotherm constants related to the heat of adsorption (J/mole), equilibrium binding constant (L/g), universal gas constant (8.314 J/mole K) and absolute temperature (K), while k_R (1/g), a_R (1/mmol) and β are the Redlich-Peterson isotherm constants. The equation may reduce to a linear isotherm at low surface coverage, and in according to Langmuir isotherm model when $\beta = 1$. The detailed parameters of these different forms of isotherm equations are listed in Table 1.

The applicability of the isotherm models was carried out by judging the correlation coefficient, R^2 values and further justified by the root-mean squared errors (RMSE), a commonly used statistical tool measuring the predictive power of a model derived as:

$$R^2 = \frac{(q_{e,meas} - \bar{q}_{e,calc})^2}{\sum (q_{e,meas} - \bar{q}_{e,calc})^2 + (q_{e,meas} - q_{e,calc})^2} \quad (8)$$

$$RMSE = \frac{\sum_{i=1}^n (q_{exp} - q_p)^2}{N_{exp} - 1} \quad (9)$$

where $q_{e,meas}$, $q_{e,calc}$ and $\bar{q}_{e,calc}$ are the measured, calculated and average mean of equilibrium uptake (mg/g), respectively, which q_{exp} (mg/g) and q_p (mg/g) are the experimental and theoretical adsorption capacity, respectively, and N is the number of experimental data points.

As provided in Table 1, Langmuir isotherm model was found satisfactory to describe the adsorption equilibrium,

Table 1
Adsorption isotherm parameters for the adsorption of ametryn onto ANC at 30°C

Isotherm models	Isotherm constants				
Langmuir	Q_o (mg/g)	K_L (L/mg)	R^2	$RMSE$	
	85.159	0.014	0.998	0.342	
Freundlich	K_F (mg/g). (L/mg) ^{1/n}	n	R^2	$RMSE$	
	3.224	1.665	0.986	2.745	
Temkin	A (L/g)	B	R^2	$RMSE$	
	0.147	18.092	0.990	1.956	
Redlich-Peterson	k_R	a_R	β	R^2	$RMSE$
	1.199	0.014	0.997	0.998	0.195

with the R^2 values higher than 0.995, as compared to the other models. The validity of the models to fit the data was support by the lowest $RMSE$ value of 0.342. The result was further justified by the β value of the Redlich-Peterson isotherm model, which approaching to the unity, indicating a Langmuir isotherm model. The findings suggested that the adsorption of ametryn onto ANC is monolayered, and the adsorption energy is distributed homogeneously throughout the surface. The results also demonstrated that each molecule poses equal enthalpies and activation energy with no transmigration of ametryn in the plane of the neighbouring surface. Table 2 lists a comparison of monolayer adsorption capacity for ametryn onto different adsorbents [46–50]. It can be concluded that the ANC prepared in this work showed relatively high monolayer adsorption capacity of 85.16 mg/g as compared to the literature. The current findings indicated the capability of ANC assisted adsorption process for the successive treatment of ametryn from the aqueous solution.

3.3. Kinetic modelling

Adsorption kinetic provides an insight into the controlling mechanism of the adsorption process, which in turn governs mass transfer and the residence time [51]. In this work, three simplified kinetic models were adopted. The pseudo-first order kinetic model [52], popularly known as the Lagergren rate expression, is represented by

$$\ln\left(\frac{q_e}{q_e - q_t}\right) = \frac{k_1}{2.303}t \quad (10)$$

where k_1 (1/h) is the pseudo-first order kinetic rate constant. Contrary to the pseudo-first order kinetic equation, pseudo-second order kinetic equation [53] predicts the behaviour over the whole range of adsorption. For the boundary conditions of $q_t = 0$ at $t = 0$ and $q_t = q_t$ at $t = t$, the Ho's kinetic model is derived as:

$$\frac{1}{(q_e - q_t)} = \frac{1}{q_e} + k_2t \quad (11)$$

where k_2 (g/mg h) is the adsorption rate constant of pseudo-second order kinetic equation. Elovich kinetic equation

Table 2
Comparison adsorption capacity for ametryn onto different adsorbents

Precursor	Modification agent	Monolayer adsorption capacity (mg/g)	Reference
Natural clay	H ₂ SO ₄	85.16	Present study
Soil	Organic matter	0.05–0.13	[46]
Chalk	–	1.55	[47]
Kaolin	–	1.82	[48]
Nano-carbon	–	105.20	[49]
Nanocomposite	Fe ₃ O ₄ /graphene	54.80	[50]

[54] is one of the most useful models describing chemisorption process given by:

$$q_t = \frac{1}{b} \ln(ab) + \frac{1}{b} \ln t \quad (12)$$

where a (mg/g h) is the initial sorption rate, and b (g/mg) is related to the extent of surface coverage and activation energy for the chemisorption process.

The experimental data for the adsorption of ametryn onto ANC at different time intervals were simulated by the pseudo-first order, pseudo-second order and Elovich kinetic models, using the plots $\ln(q_e - q_t)$ against t , t/q_t versus t , and q_t against $\ln t$, respectively. The corresponding results are tabulated in Table 3. The suitability of the kinetic model to describe the adsorption process was ascertained by the value of correlation coefficient, R^2 and the normalized standard deviation, Δq (%) derived as:

$$\Delta q (\%) = 100 \sqrt{\frac{\sum |(q_{e,exp} - q_{e,calc}) / q_{e,exp}|^2}{n - 1}} \quad (13)$$

where n is the number of data points, $q_{e,exp}$ (mg/g) and $q_{e,calc}$ (mg/g) are the experimental and calculated adsorption capacities, respectively. The correlation coefficients obtained for the pseudo-first order and Elovich kinetic models were relatively low, and the experimental q_e values did not agree satisfactory with the calculated values. Good agreement was shown between the experimental data with the pseudo-second order kinetic model, with the $R^2 > 0.99$ and the lowest normalized standard deviation, Δq (%) values, which ranged between 2.64 to 14.01%. This result suggested that the adsorption system followed the pseudo-second order kinetic model, based on the assumption that the rate-limiting step may be chemisorption process.

3.4. Adsorption mechanism

To gain further insight into the mechanism and rate-controlling steps affecting the adsorption process, the intra-particle diffusion model [55] has been elucidated as:

$$q_t = k_{pi}t^{1/2} + C_i \quad (14)$$

Table 3
Adsorption kinetic parameters for the adsorption of ametryn onto ANC at 30°C

C_0 (mg/L)	$q_{e,exp}$ (mg/g)	Pseudo-first order				Pseudo-second order				Elovich				
		$q_{e,cal}$ (mg/g)	k_1 (1/h)	R^2	Δq (%)	$q_{e,cal}$ (mg/g)	k_2 (g/mg h)	R^2	Δq (%)	$q_{e,cal}$ (mg/g)	a (mg/g h)	b (g/mg)	R^2	Δq (%)
25	12.49	7.80	1.676	0.687	37.55	12.82	0.167	0.995	2.64	8.64	53.82	0.327	0.993	30.83
50	23.22	16.86	2.116	0.972	27.39	24.69	0.097	0.995	6.33	17.64	116.91	0.172	0.991	24.03
75	32.66	23.68	2.133	0.957	27.48	33.90	0.078	0.998	3.80	24.56	130.15	0.106	0.995	24.80
100	38.89	27.63	1.849	0.956	28.95	40.00	0.061	0.991	2.85	28.26	192.39	0.106	0.986	27.33
125	44.77	29.66	1.638	0.899	33.75	46.30	0.044	0.997	3.42	31.14	189.29	0.092	0.995	30.44
150	50.12	34.03	1.761	0.920	32.11	57.14	0.029	0.990	14.01	35.43	193.16	0.076	0.989	29.31

where k_p is the intra particle diffusion rate constant ($\text{mg/g}\cdot\text{h}^{1/2}$), and C_i is the intercept of stage i , which can be evaluated from the intercept and slope of the plot of q_t versus $t^{1/2}$. Generally, the adsorption process is considered to involve three major steps: (i) mass transfer across the external boundary layer film of liquid surrounding the outside of the particle; (ii) adsorption onto the adsorbent surface (internal or external); and (iii) diffusion of the adsorbate molecules into the adsorption sites either by a pore diffusion process through the liquid filled pores or by a solid surface diffusion mechanism [56]. The first, sharper portion was attributed to the diffusion of ametryn from the aqueous solution to the external surface of adsorbent, or the boundary layer diffusion of the solute molecules. The second portion represents the gradual adsorption stage, where intraparticle diffusion was rate limiting step. The last portion was the final equilibrium stage which intraparticle diffusion started to slow down due to the extremely low ametryn concentration left in the solution.

From Fig. 2, the plots presents multi-linearity steps, implying that more than one steps has affected the adsorption mechanism. According to the model, if the intraparticle diffusion was the sole rate-controlling step, the plot would pass through the origin. The values of the intra-particle diffusion rate constant (Table 4) were determined by fitting the experimental data with the intra particle equation. The first stage can be referred to the diffusion of ametryn to the external surface of ANC, a process known as boundary layer diffusion. The high k_{p1} value, 9.02–35.78 $\text{mg/g h}^{1/2}$ of the first stage indicates that the adsorption rate was high when time tended towards zero [57]. The second stage demonstrated gradual adsorption, whereby intra-particle diffusion was the rate-limiting step, due to the lower values of k_{p2} of 3.71–11.69 $\text{mg/g h}^{1/2}$. During this stage, the ametryn molecules would gradually occupy the external surface of ANC and the driving force ceased to maintain the external mass transfer. At the last stage, almost all pores in the adsorbent were occupied by ametryn molecules, external mass transfer would drastically decrease, and there were virtually no film or intra-particle diffusions. This represents the dynamic equilibrium of the adsorption process, which the k_{p3} values are at a minimum value. Meanwhile it is worth noting that the second- and third-stage lines passed away from the origin, indicating that the rate-limiting step of the adsorption process was not solely governed by the intra-particle diffusion mechanism [58].

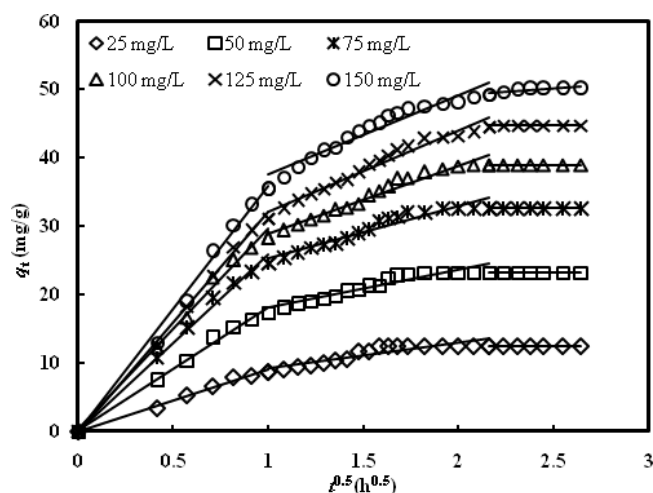


Fig. 2. Plots of intraparticle diffusion model for the adsorption of ametryn onto ANC at 30°C.

3.5. Adsorption thermodynamic

For clarification on the dominating mechanism of the adsorption process, it is important to take into the account about the thermodynamic behaviour of the liquid-solid system. Adsorption thermodynamic allows a better understanding on the adsorption phenomenon, and the design of the adsorption system [59]. The distribution coefficients, K_d is defined as C_{Ae} , the amount adsorbed on solid phase at equilibrium (mg/L) divided by C_e , the concentration in the liquid phase (mg/L), and the free Gibbs energy, ΔG° (kJ/mole) of the adsorption process is derived as:

$$K_d = \frac{C_{Ae}}{C_e} \quad (15)$$

$$\Delta G^\circ = -RT \ln K_d \quad (16)$$

The values of ΔH° and ΔS° were deduced from the slope and intercept of the van't Hoff plot of $\ln K_d$ vs. $1/T$, using the expression given by:

$$\ln K_d = \frac{\Delta S^\circ}{R} - \frac{\Delta H^\circ}{RT} \quad (17)$$

Table 4
Intraparticle diffusion model parameters for the adsorption of ametryn onto ANC at 30°C

C_0 (mg/L)	Intraparticle diffusion model			C_1	C_2	C_3	$(R_1)^2$	$(R_2)^2$	$(R_3)^2$
	k_{p1} (mg/g h ^{1/2})	k_{p2} (mg/g h ^{1/2})	k_{p3} (mg/g h ^{1/2})						
25	9.021	3.711	–	0	5.481	12.488	0.9902	0.8205	–
50	18.173	5.563	–	0	12.441	23.216	0.9930	0.9099	–
75	25.908	7.692	–	0	17.596	32.661	0.9916	0.9282	–
100	29.621	9.986	–	0	18.864	38.879	0.9920	0.9635	–
125	31.947	11.763	0.256	0	20.381	44.125	0.9969	0.9701	0.3459
150	35.784	11.686	1.595	0	25.784	46.098	0.9918	0.9701	0.6718

Table 5
Thermodynamic parameters for the adsorption of ametryn onto ANC

ΔG° (kJ/mole)			ΔH° (kJ/mole)	ΔS° (J/mole K)
30°C	40°C	50°C		
–90.692	–16.528	66.901	–2.477	8.305

where ΔS° and ΔH° are denoted as the standard entropy change and enthalpy change, respectively. The calculated thermodynamic parameters at the operating temperatures of 30, 40, and 50°C, respectively are listed in Table 5. The negative value of ΔH° indicated that the adsorption process was exothermic in nature. The positive values of ΔS° showed the high affinity of ANC for ametryn, and the increasing randomness at the solid-solution interface, with some structural changes in the adsorbates and adsorbents during the adsorption process.

The negative values of ΔG° indicated spontaneous nature of the adsorption process at the temperature range being studied, while the rising value of ΔG° showed that the given process was less favourable at the higher sorption temperatures of 40 and 50°C. The increasing positivity of ΔG° is related to the surface tension of the adsorbent minimizing their respective surface area. Increasing temperature led to the decrease of ametryn uptake, due to higher repulsive forces between the active sites of ANC and the ametryn species, and between the adjacent ametryn molecules. Higher operating temperatures may enhance the solubility of the ametryn molecules, and the desorption rate in the adsorption mechanism. Therefore, the solute molecules were more difficult to be adsorbed. As a result, an extra surface free energy is required to extend the surface area by stretching, or distorting their respective surface. The finding was consistent with the experimental data recorded by Yamane and Green [34], which reported that the adsorptive uptake of ametryn increased with decreasing the operating temperature from 25 to 15°C. The phenomenon has also been observed in the adsorption of carbofuron onto maize cob at the high operating temperature of 50°C [60].

3.6. Textural, functional and surface characterizations

Scanning electron microscopy (SEM) has been a primary tool to examine the surface morphology and funda-

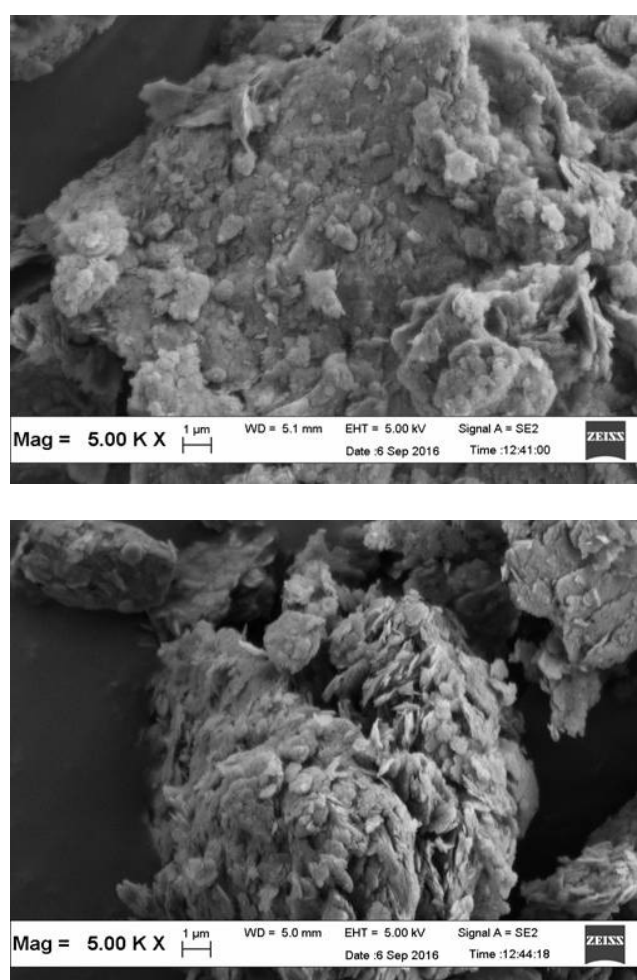


Fig. 3. Scanning electron micrographs of (a) NC and (b) ANC.

mental physical properties of the adsorbents. It is useful for the determination of the particle shape, porosity and appropriate pore size distribution of the functionalized adsorbents. SEM measures the surface morphology of conducting and non-conducting materials by analyzing the back scattered electron (BSE) and secondary electron (SE). The SEM images of the raw natural clay (NC) and ANC are depicted in Fig. 3. NC demonstrated a dense structure with

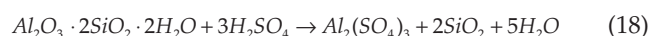
the presence of humps and platy flakes around the surface [61]. However, ANC displayed a highly compact morphology, with a variety of macro and meso porosities surrounding the surface.

The FTIR analysis was carried out for the identification of surface functional groups present on the adsorbent surface. The FTIR spectra of the natural clay (NC), acid treated natural clay (ANC) and ametryn loaded ANC is illustrated in Fig. 4. The broad peak at 3600–3200 cm^{-1} can be assigned to the stretching mode of hydroxyl groups with hydrogen bonding. The bands at 1646–1634, 1031–1007, 912, 796–749, 695–694, 535, and 472–470 cm^{-1} , respectively may be attributed to the –OH bending, Si–OH stretching, Al–OH–Al, Al–Mg–OH, –OH, Si–O–Al deformation and Si–O–Si functionalities.

Generally, acid treatment is related to the penetration of protons and dihydroxylation reaction connected with the successive dissolution of the central atoms and the alteration of absorption bands [62]. A slight shift of the wavenumbers showed a higher asymmetry of ANC, favouring the formation of cationic defects on the bulk structure (dissolution of carbonates and feldspars, removal of cations from the interlayer spacing, leaching of the octahedral cations and the complete destruction of the clay structure). In the O–H stretching region, the untreated and treated clays showed two predominant bands at 3697 cm^{-1} and 3621 cm^{-1} corresponding to the inner hydroxyl groups, lying between the tetrahedral and octahedral sheets. A lower structural hydroxyl vibration band for ANC verified the successive leaching of the Al^{3+} cations from the octahedral layer during the modification process [63]. The strong band in the 1120–1000 cm^{-1} region is due to Si–O stretching in the natural clay, that has been altered in shape and position after acid treatment, due to the structural modification in the tetrahedral cations. A lower intensity of the absorption bands at 912 and 749 cm^{-1} for ANC suggested the partial reduction of Al^{3+} and Fe^{2+} from the clay structure. The presence of a new peak at 795–802 cm^{-1} is mainly due to the formation of free amorphous silica during the destruction of the tetrahedral sheets [64]. According to Krupskaya et al. [65], the protonation of Al bond pairs in the octahedron sheets may transform the tetrahedral sheets from 4-coordination to 6-coordination, with the alteration of the layer stacking and formation of mesoporous structure. In contrast, the

presence of an intensive peak at 1646 cm^{-1} in the ametryn loaded ANC may be ascribed to the adsorption of ametryn onto the ANC surface through hydrogen bondings. Similar result has been reported by Davies and Jabeen [4] on the adsorption of atrazine onto the clay minerals and soils.

The interactions of low polarity vapours with soil colloids and clay minerals are governed to a large extent by the porosities of the solid adsorbents, which are reflected by the surface physical properties evaluated using an inert gas [66]. Table 6 summarizes the surface physical parameters of NC and ANC. The BET surface area, Langmuir surface area, total pore volume and average pore size of the raw NC were identified to be 32.31 m^2/g , 41.50 m^2/g , 0.112 cm^3/g , and 148.93 Å, respectively. However, ANC demonstrated the BET surface area, Langmuir surface area, total pore volume and average pore size of 43.34 m^2/g , 55.80 m^2/g , 0.120 cm^3/g and 102.95 Å, respectively, implying pore development during the modification stage. The chemical modification for the dissolution of metal components could be best represented by the reaction:



According to Hassan and El-Shall [67], acid treatment would induce leaching of octahedral sheets, with the structural rearrangement and development of mesopores throughout the surface. The rising surface area could be related to the channel cleansing, but more likely, due to the elimination of aggregates impurities from the octahedral cations of the clay minerals [68]. From the nitrogen adsorption isotherm analysis (Fig. 5), it was inferred that the isotherm of ANC belong to type IV isotherm as defined by the International Union of Pure and Applied Chemistry (IUPAC) classification. This type of isotherm is usually exhibited by the presence of mesoporous structure. Meanwhile, the desorption branch presents a hysteresis loop at high relative pressures, pointing to a considerable development of mesoporosity [69,70].

4. Conclusion

The preparation of a low cost and eco-friendly functionalized adsorbent from the natural clay has been presented. Acid modification has altered the octahedral sheets, and improved the specific surface area, reflected by the for-

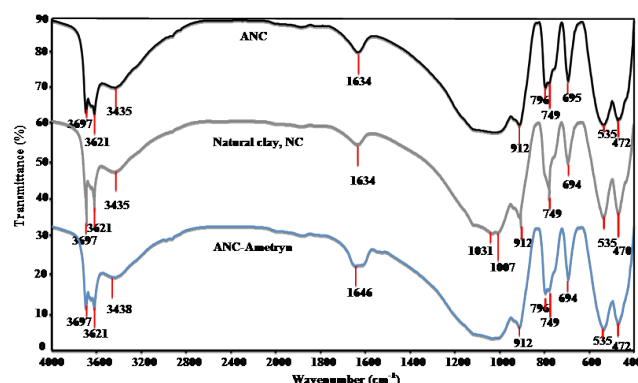


Fig. 4. FTIR spectra of natural clay (NC), ANC and ametryn loaded ANC.

Table 6
Surface physical parameters of ANC

Properties	NC	ANC
BET surface area (m^2/g)	32.31	43.34
Micropore surface area (m^2/g)	3.33	4.01
External surface area (m^2/g)	28.98	39.34
Langmuir surface area (m^2/g)	41.50	55.80
Total pore volume, (cm^3/g)	0.112	0.120
Micropore volume (cm^3/g)	0.002	0.001
Mesopore volume (cm^3/g)	0.110	0.119
Average pore size (Å)	148.93	102.95

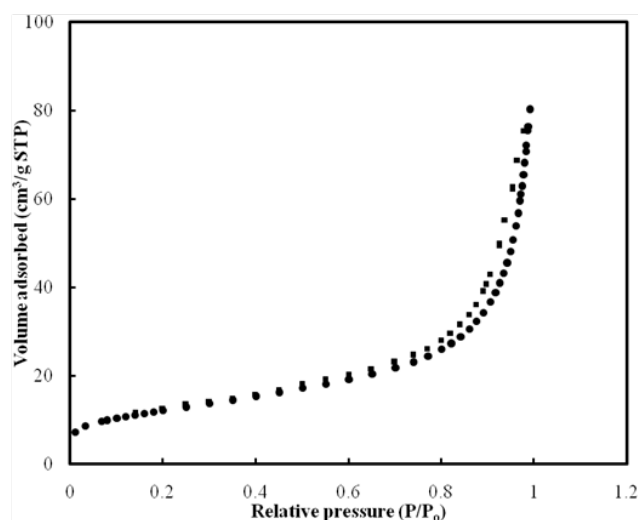


Fig. 5. Nitrogen adsorption-desorption curve of ANC.

mation of new pores, and corroborated well with the SEM findings. The FTIR spectra verified the new development of surface functionalities. The adsorptive behaviour for the remediation of ametryn has been examined. The adsorption data were best represented by the Langmuir isotherm model, and the adsorption kinetic was fitted closely to the pseudo-second order kinetic model, with a monolayer adsorption capacity for ametryn of 85.16 mg/g. The adsorption process was found to be dependent on the solution pH, favouring the adsorption uptake of ametryn onto ANC at the acidic conditions. The negative ΔH° illustrated exothermic nature of the adsorption interaction, while positive ΔS° verified the increased randomness at the solid-solution interface. The findings ascertained the potential of ANC as a viable solution for the adsorptive treatment of ametryn contaminated agricultural runoff.

Acknowledgement

The authors acknowledge the financial support provided by the Ministry of Higher Education of Malaysia and Universiti Sains Malaysia under the Research University (RUI) (Project No. 1001/PREDAC/814272) and FRGS (Project No. 304/PREDAC/6171157) research grant schemes.

References

- [1] K. Schiff, M. Sutula, Organophosphorus pesticides in storm-water runoff from Southern California (USA), *Environ. Toxicol. Chem.*, 23 (2004) 1815–1821.
- [2] T.D. Bucheli, S.R. Müller, S. Heberle, R.P. Schwarzenbach, Occurrence and behaviour of pesticides in rainwater, roof runoff, and artificial stormwater infiltration, *Environ. Toxicol. Chem.*, 32 (1998) 3457–3464.
- [3] C.D. Brown, J.M. Hollis, SWAT- A semi-empirical model to predict concentrations of pesticides entering surface waters from agricultural land, *Pestic. Sci.*, 47 (1996) 41–50.
- [4] J.E.D. Davies, N. Jabeen, The adsorption of herbicides and pesticides on clay minerals and soils. Part 2. Atrazine, *J. Inclusion Phenom. Macrocylic Chem.*, 46 (2003) 57–64.
- [5] H. Mabrouki, D.E. Akretche, Diclofenac potassium removal from water by adsorption on natural and pillared clay, *Desal. Water Treat.*, 57 (2016) 6033–6043.
- [6] R.H.S. Robertson, Fuller's Earth: A history of calcium montmorillonite, Mineralogical Society occasional publication, Volturna Press, Hythe, Kent, 1986.
- [7] M.I. Carretero, C.S.F. Gomes, F. Tateo, In: F. Bergaya, B.K.G. Theng, G. Lagaly, Handbook of clay science, Elsevier, Amsterdam 2006, pp. 717–742.
- [8] M.-T. Droy-Lefaix, F. Tateo. In: F. Bergaya, B.K.G. Theng, G. Lagaly, Handbook of clay science, Elsevier, Amsterdam 2006, pp. 743–752.
- [9] E. Lund, B. Nissen, Low technology water purification by bentonite clay flocculation as performed in Sudanese villages. *Virological examinations, Water Res.*, 20 (1986) 37–43.
- [10] M. Madsen, J. Schlundt, Low-technology water purification by bentonite clay flocculation as performed in Sudanese villages: Bacteriological examinations, *Water Res.*, 23 (1989) 873–882.
- [11] M.M. Mortland, Clay-organic complexes and interactions, *Adv. Agron.*, 22 (1970) 75–117.
- [12] Z. Ullah, S. Hussain, S. Gul, S. Khan, F.K. Bangash, Use of HCl-modified bentonite clay for the adsorption of Acid Blue 129 from aqueous solutions, *Desal. Wat. Treat.*, 57 (2016) 8894–8903.
- [13] S. Wang, N. Qiao, J. Yu, X. Huang, M. Hu, H. Ma, Effect of ionic strength on the adsorption behavior of phenol over modified activated clay, *Desal. Wat. Treat.*, 57 (2016) 4174–4182.
- [14] N. Abidi, J. Duplay, E. Errais, A. Jada, M. Trabelsi-Ayadi, Discoloration of textile effluent by natural clay improved through the presence of dyeing additives, *Desal. Wat. Treat.*, 57 (2016) 27954–27968.
- [15] G. Lagaly, M. Ogawa, I. Dékány, In: F. Bergaya, B.K.G. Theng, G. Lagaly, Handbook of clay science, Elsevier, Amsterdam 2006, pp. 309–379.
- [16] H. van Olphen, An introduction to clay colloid chemistry, Wiley Interscience, 1977.
- [17] K.G. Bhattacharyya, S.S. Gupta, Adsorption of a few heavy metals on natural and modified kaolinite and montmorillonite: A review, *Adv. Colloid Interface. Sci.*, 140 (2008) 114–131.
- [18] B.A. Fil, C. Özmetin, M. Korkmaz, Characterization and electrokinetic properties of montmorillonite, *Bulgarian Chem. Commun.*, 46 (2014) 258–263.
- [19] E.L. Foletto, C. Volzone, L.M. Porto, Performance of an Argentinian acid-activated bentonite in the bleaching of soybean oil, *Braz. J. Chem. Eng.*, 20 (2003) 139–145.
- [20] J.P. Nguetnkam, R. Kamga, F. Villiéras, G.E. Ekodeck, J. Yvon, Assessing the bleaching capacity of some Cameroonian clays on vegetable oils, *Appl. Clay Sci.*, 39 (2008) 113–121.
- [21] B. Paul, D. Yang, X. Yang, X. Ke, R. Frost, H. Zhu, Adsorption of the herbicide simazine on moderately acid-activated beidellite, *Appl. Clay Sci.*, 49 (2010) 80–83.
- [22] A.K. Panda, B.G. Mishra, D.K. Mishra, R.K. Singh, Effect of sulphuric acid treatment on the physico-chemical characteristics of kaolin clay, *Colloids Surfaces A: Physicochem. Eng. Aspects* 363 (2010) 98–104.
- [23] N. Frini-Srasra, E. Srasra, Determination of acid-base properties of HCl acid activated palygorskite by potentiometric titration, *Surf. Eng. Appl. Electrochem.*, 44 (2008) 401–409.
- [24] C. Belver, M.A.B. Munoz, M.A. Vicente, Chemical activation of a kaolinite under acid and alkaline conditions, *Chem. Mater.* 14 (2002) 2033–2043.
- [25] M.S. El-Geundi, T.E. Farrag, H.M.A. El-Ghany, Adsorption equilibrium of a herbicide (pendimethalin) onto natural clay, *Adsorpt. Sci. Technol.*, 23 (2005) 437–453.
- [26] G.M. Ratnamala, S.K. Vidya, G. Srinikethan, Isotherm, kinetics, and process optimization for removal of remazol Brilliant Blue dye from contaminated water using adsorption on acid-treated red mud, *Desal. Wat. Treat.*, 57 (2016) 11361–11374.
- [27] F. Abidar, M. Morghi, A. Ait Ichou, A. Soudani, M. Chiban, F. Sinan, M. Zerbet, Removal of orthophosphate ions from aqueous solution using chitin as natural adsorbent, *Desal. Wat. Treat.*, 57 (2016) 14739–14749.

- [28] B.A. Fil, C. Ozmetin, Adsorption of cationic dye from aqueous solution by clay as an adsorbent: Thermodynamic and kinetic studies, *J. Chem. Soc. Pak.*, 34 (2012) 896–906.
- [29] B.A. Fil, Isotherm, kinetic, and thermodynamic studies on the adsorption behavior of malachite green dye onto montmorillonite clay, *Part. Sci. Technol.*, 34 (2016) 118–126.
- [30] Y. Shang, J. Zhang, X. Wang, R. Zhang, W. Xiao, S. Zhang, R. Han, Use of polyethyleneimine-modified wheat straw for adsorption of Congo Red from solution in batch mode, *Desal. Wat. Treat.*, 57 (2016) 8872–8883.
- [31] J.B. Weber, Molecular structure and pH effects on the adsorption of 13 s-triazines compound on montmorillonite clay, *Am. Mineral.*, 51 (1966) 1657–1670.
- [32] R. Ahmad, R.S. Kookana, A.M. Alston, Sorption of ametryn and imazethapyr in twenty-five soils from Pakistan and Australia, *J. Environ. Sci. Health., Part B*, 36 (2001) 143–160.
- [33] R.E. Green, Pesticides in soil and water, Soil Science Society of America, Wisconsin, Inc., Madison, 1974.
- [34] V.K. Yamane, R.E. Green, Adsorption of ametryne and atrazine on an oxisol, montmorillonite, and charcoal in relation to pH and solubility effects, *Soil Sci. Soc. Am. J.*, 36 (1972) 58–64.
- [35] Y. Yang, Y. Chun, G. Sheng, M. Huang, pH-dependence of pesticide adsorption by wheat-residue-derived black carbon, *Langmuir*, 20 (2004) 6736–6741.
- [36] R.J. Hance, Influence of pH, exchangeable cation and the presence of organic matter on the adsorption of some herbicides by montmorillonite, *Can. J. Soil Sci.*, 49 (1969) 357–364.
- [37] J. Weber, Mechanism of adsorption of s-triazines by clay colloids and factors affecting plant availability, *Residue Rev.*, 32 (1970) 93–130.
- [38] H. Van Olphen, An introduction to clay colloid chemistry, Interscience, New York, 1963.
- [39] C.T. Johnston, E. Tombácz, In: J.B. Dixon, D.G. Schulze, Soil mineralogy with environmental applications, *Soil Sci. Soc. Am.*, Madison, WI, 2002, pp. 37–67.
- [40] E. Tombácz, M. Szekeres, Colloidal behavior of aqueous montmorillonite suspensions: The specific role of pH in the presence of indifferent electrolytes, *Appl. Clay Sci.*, 27 (2004) 75–94.
- [41] P. Phatai, C.M. Futralan, Removal of methyl violet dye by adsorption onto mesoporous mixed oxides of cerium and aluminium, *Desal. Wat. Treat.*, 57 (2016) 8884–8893.
- [42] I. Langmuir, The adsorption of gases on plane surfaces of glass, mica and platinum, *J. Am. Chem. Soc.*, 40 (1918) 1361–1403.
- [43] H.M.F. Freundlich, Over the adsorption in solution, *J. Phys. Chem.*, 57 (1906) 385–471.
- [44] M.I. Tempkin, V. Pyzhev, Kinetics of ammonia synthesis on promoted iron catalysts, *Acta Physicochim URSS*, 12 (1940) 217–222.
- [45] O. Redlich, D.L. Peterson, A useful adsorption isotherm, *J. Phys. Chem.*, 63 (1959) 1024–1026.
- [46] C. Slusznzy, E.R. Graber, Z. Gerst, Sorption of s-triazine herbicides in organic matter amended soils: Fresh and incubated systems, *Water Air Soil Pollut.*, 115 (1999) 395–410.
- [47] A. Wefer-Roehl, E.R. Graber, M.D. Borisover, E. Adar, R. Nativ, Z. Ronen, Sorption of organic contaminants in a fractured chalk formation, *Chemosphere*, 44 (2001) 1121–1130.
- [48] Q. Wang, A.T. Lemley, Reduced adsorption of ametryn in clay, humic acid, and soil by interaction with ferric ion under fenton treatment conditions, *J. Environ. Sci. Health., Part B*, 41 (2006) 223–236.
- [49] M.C. Prete, F.M. de Oliveira, C.R.T. Tarley, Assessment on the performance of nano-carbon black as an alternative material for extraction of carbendazim, tebutiuron, hexazinone, diuron and ametryn, *J. Environ. Chem. Eng.*, 5 (2017) 93–102.
- [50] P.K. Boruah, B.Sharma, N. Hussain, M.R. Das, Magnetically recoverable Fe₃O₄/graphene nanocomposite towards efficient removal of triazine pesticides from aqueous solution: Investigation of the adsorption phenomenon and specific ion effect, *Chemosphere*, 168 (2017) 1058–1067.
- [51] L. Khezami, K.K. Taha, E. Amami, I. Ghiloufi, L. El Mir, Removal of cadmium(II) from aqueous solution by zinc oxide nanoparticles: Kinetic and thermodynamic studies, *Desal. Water Treat.*, 62 (2017) 346–354.
- [52] S. Lagergren, B.K. Svenska, Zur theorie der sogenannten adsorption geloeester stoffe, *Veternskapsakad Handlingar*, 24 (1898) 1–39.
- [53] Y.S. Ho, G. McKay, The kinetics of sorption of basic dyes from aqueous solutions by sphagnum moss peat, *Can. J. Chem. Eng.*, 76 (1998) 822–827.
- [54] C. Aharoni, F.C. Tompkins, In: D.D. Eley, H. Pines, P.B. Weisz, Advances in catalysis and related subjects, Academic Press, New York 1970, pp. 1–49.
- [55] W.J. Weber, J.C. Morris, Kinetics of adsorption on carbon from solution, *J. Sanit. Eng. Div. Am. Soc. Civ. Eng.*, 89 (1963) 31–60.
- [56] W.H. Cheung, Y.S. Szeto, G. McKay, Intraparticle diffusion processes during acid dye adsorption onto chitosan, *Biore-sour. Technol.*, 98 (2007) 2897–2904.
- [57] O. Pezoti, A.L. Cazetta, I.P.A.F. Souza, K.C. Bedin, A.C. Martins, T.L. Silva, V.C. Almeida, Adsorption studies of methylene blue onto ZnCl₂-activated carbon produced from buriti shells (*Mauritia flexuosa* L.), *J. Ind. Eng. Chem.* 20 (2014) 4401–4407.
- [58] M.H. Marzbali, M. Esmaili, H. Abolghasemi, M.H. Marzbali, Tetracycline adsorption by H₃PO₄-activated carbon produced from apricot nut shells: A batch study, *Process Saf. Environ. Prot.*, 102 (2016) 700–709.
- [59] A. Nakhli, M. Bergaoui, C. Aguir, M. Khalfaoui, M.F. M'henni, A.B. Lamine, Adsorption thermodynamics in the framework of the statistical physics formalism: Basic Blue 41 adsorption onto *Posidonia* biomass, *Desal. Water Treat.*, 57 (2016) 12730–12742.
- [60] K.Y. Foo, Value-added utilization of maize cobs waste as an environmental friendly solution for the innovative treatment of carbofuron, *Process Saf. Environ. Prot.*, 100 (2016) 295–304.
- [61] S. Sahoo, Uma, S. Banerjee, Y.C. Sharma, Application of natural clay as a potential adsorbent for the removal of a toxic dye from aqueous solutions, *Desal. Wat. Treat.*, 52 (2014) 6703–6711.
- [62] F. Gomri, M. Boutahala, H. Zaghoulane-Boudiaf, S.A. Korili, A. Gil, Removal of Acid Blue 80 from aqueous solutions by adsorption on chemical modified bentonites, *Desal. Water Treat.*, (2016) 1–10.
- [63] J. Madejova, FTIR Techniques in clay mineral studies, *Vib. Spectrosc.* 31 (2003) 1–10.
- [64] B.N. Dudkin, I.V. Loukhina, E.G. Avvakumov, V.P. Isupov, Application of mechanochemical treatment of disintegration of kaolinite with sulphuric acid, *Sust. Dev.*, 12 (2004) 327–330.
- [65] V.V. Krupskaya, S.V. Zakusin, E.A. Tyupina, O.V. Dorzhieva, A.P. Zhukhlistov, P.E. Belousov, M.N. Timofeeva, Experimental study of montmorillonite structure and transformation of its properties under treatment with inorganic acid solutions, *Minerals*, 7 (2017) 1–15.
- [66] S. Brunauer, P.H. Emmett, E. Teller, Adsorption of gases in multimolecular layers, *J. Am. Chem. Soc.*, 60 (1938) 309–319.
- [67] M. Hassan, H. El-Shall, Texture and microstructure of thermally-treated acid-leached kaolinitic clays, *Adsorpt. Sci. Technol.*, 27 (2009) 671–684.
- [68] R.N. Oliveira, W. Acchar, G.D.A. Soares, L.S. Barreto, The increase of surface area of a Brazilian palygorskite clay activated with sulfuric acid solutions using a factorial design, *Mater. Res.*, 16 (2013) 924–928.
- [69] K.S.W. Sing, D.H. Everett, R.A.W. Haul, L. Moscou, R.A. Pierotti, J. Rouquerol, T. Siemieniewska, Reporting physisorption data for gas/solid systems with special reference to the determination of surface area and porosity, *Pure Appl. Chem.*, 57 (1985) 603–609.
- [70] K.Y. Foo, B.H. Hameed, Porous structure and adsorptive properties of pineapple peel based activated carbons prepared via microwave assisted KOH and K₂CO₃ activation, *Micropor. Mesopor. Mater.*, 148 (2012) 191–195.